Fe-Ni-S COMPOSTIONS AFTER BACKGROUND CORRECTION: AN ONGOING STUDY OF THE PROPERTIES OF WILD 2 SMALLEST SULFIDE GRAINS IN QUENCHED SUPERHEATED AEROGEL.

Frans J. M. Rietmeijer, Department of Earth and Planetary Sciences, MSC03 2040, 1-University of New Mexico, Albuquerque, NM 87131-0001, USA; e-mail: fransjmr@unm.edu

Introduction: There are two different but not mutually exclusive reasons to analyze Stardust samples, (1) understanding the mineral and chemical properties of dust from a known Kuiper Belt comet for signatures of solar nebula and molecular cloud dust, and (2) understanding the hypervelocity capture-induced modifications of comet Wild 2 dust particles, *i.e.* the performance of underdense aerogel that might be used on future dust-capture missions. I doubt any Wild 2 grains survived with their original properties fully intact and certainly most of the nanometer grains were texturally and chemically modified. The Fe-Ni-S compound textures, *incl*. discontinuous chemical zoning, and their distribution pattern in quenched silica aerogel melt were reproduced in a hypervelocity impact experiment using micrometer pyrrhotite grains [1].

The model: The nanometer scale Wild 2 dust particles that encountered superheated aerogel [2] disintegrated instantaneously into a chaotic mixture of fragments, melt droplets, vapor, and neutral and charged atoms that quenched via metastable eutectic vapor condensation and liquidus-controlled reactions that produced porous clumps of vesicular Si-rich glass.

I report on initial results of background-corrected Fe-Ni-S compositions obtained by ATEM analyses in Si-rich clumps from two tracks and emerging trends on compositions established during hypervelocity capture.

Aerogel background: The vesicular glass matrix is not pure SiO_2 but contains minor Na, Mg, Al, S, Cl, K, Ca, Cr, Mn, Fe and Ni that are the elevated concentrations of these elements in pre-flight aerogel. It forms a persistent background in this matrix [3]. The silica-rich glass, Fe-Ni-S and silicate inclusions after interacting with superheated silica aerogel must be corrected for this background [3, 4]. Its Fe:Ni:S (at) proportions are 73:15:12 [2], but what controls this background? There are no high-Si eutectics in the Fe-Si, Ni-Si and S-Si phase diagrams to support liquidus or metastable eutectic control. Such high-Si eutectics cannot be entirely ruled that would yield Fe:Ni:S (at) = 60:20:20. The Fe:S background ratio is defined by deep metastable Fe-S eutectics [5] that emerged during quenching. The background correction acts as a filter to reduce data scatter. It is most dramatic for Ni, *i.e*. many measured Fe-Ni-S compositions loose all Ni (and most Cr and Mn, ref. 3).

Fe-Ni-S compositions: The majority of Fe-S grains in allocation C2092,2,80,47,6 is Ni-free; Ni is in metal and low-S (<30 at%) grains; mean ± S.D = 3 ± 1.6 Ni at% (Fig. 1). The compound compositions, 40<S<60 (at), include three Fe-S populations (1) 46 ± 5, (2) 53 and (3) 57 ± 2.5 at%, straddling the $Fe_{1-x}S$ congruent melting point at 1190°C. The 40<S<60 (at) compositions are very well constrained on the liquidus in the Fe-S phase diagram (Fig. 1).

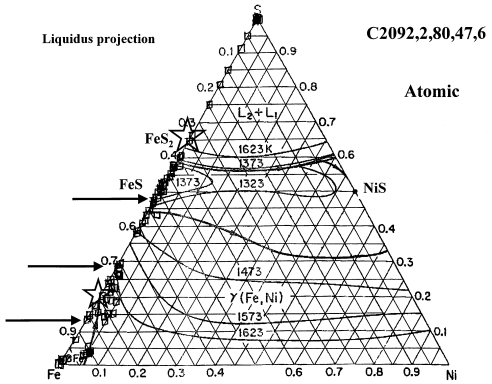

Figure 1: Liquidus projection of the Fe-Ni-S (at) diagram (after ref. 6) with the background-corrected grain compositions in aerogel of allocation C2092,2,80,47,6. Three deep metastable Fe-S eutectics are indicated (after ref. 5; arrows)

Compositions, S>65 (at), include FeS_2 (no electron diffraction confirmation) and amorphous Fe-S grains. The pure sulfur (<1 at) spots are residuals after background correction. The gap between 30-40 S at% (Fig. 1) separates (1) Fe,Ni and low-S (<30 at) Fe-Ni-S grains cooling from the Fe melting point (1539°C) and (2) Fe-S melts at 1190°C. It also suggests deep metastable eutectic behavior of low-S Fe-Ni-S grains (Fig. 1; arrows) but liquidus control of Ni-free FeS compounds.

Fe-Ni-S compositions vs. Si (at): Using allocation C2004,1,44,1,3 [5] as an example, Mg in silica glass is either (1) aerogel background for Si<15 (at) or (2) background and Mg from Mg,Fe-silicates when 15 <Si <31 (at) (Fig. 2). Open stars in the Fe-Ni-S diagram (inset) are for FeS_2 and the low-S Fe-Ni-S cotectic line at the Fe-S join. Both are plausible chemical markers.

The background corrected Fe-S and Fe-Ni-S compositions, S<20 and 30<S<65 (at), in the part of the diagram between 15 and 31 Si (at%) in allocation C2054,0,35,44,6 are identical to the sulfide compositions at Si<15 (at). Thus, Fe from Fe,Mg-silicates was not partitioned in the Fe-S and Fe-Ni-S compounds as a function of mixing with SiO_2 melt .

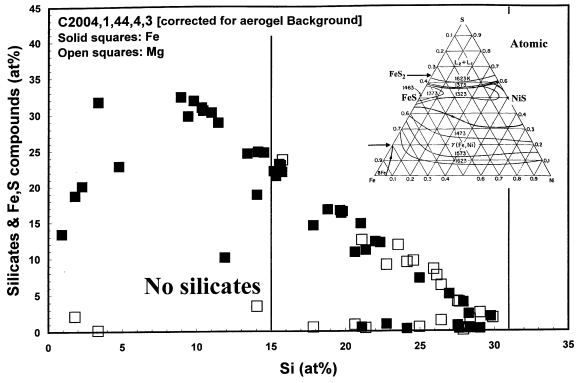

Figure 2: Background corrected atomic Mg and Fe contents vs. Si showing mixing of Fe-Ni-S and silicate grains with silica aerogel in allocation C2004,1,44,4,3 [5]. Mg in glass Si<15) may be MgS [7]; Fe-silicide spheres are present. Inset: Fe-Ni-S ternary diagram modified after ref. [6].

The Fe-Ni-S compositions in this allocation (Fig. 3) resemble those shown in Fig. 1 but without the gap. They also have three Fe-S populations (1) 47 ± 3, (2) 54 and (3) 60 at%. The pure sulfur 'hot spots' contain up to 9.5 at% S. There are a few Fe-S grains with a stoichiometric FeS_2 composition and S = 80 at%, *i.e.* corner-shared FeS_4 tetrahedra [8]. FeS_2 and FeS_4 compositions were found in several glass allocations.

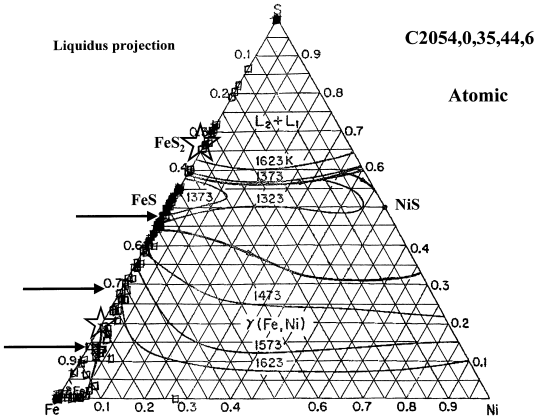

Figure 3: Fe-Ni-S (at) diagram (*cf.* Fig. 1) with background corrected grain compositions in allocation C2054,0,35,44,6.

Zoning: The discontinuously zoned Fe-S grains in allocation C2054,0,35,44,6 can be, *incl*. (1) a core with a narrow rim and a long 'tail', (2) a core with a well developed rim, and (3) dumbbell shaped grains (Table 1).

Table 1: Core-'rim' relationships in discontinuously zoned Fe-Ni-S and Fe-S grains in allocation C2054,0,35,44,6.

	Core	**'rim'**
Grain/tail	$Fe_{87}S_{13}$	$Fe_{49}S_{51}$
Grain/rim	$Fe_{78.5}Ni_3S_{18.5}$	$Fe_{58}S_{42}$
Dumbbell grain	Fe_{89} Ni_1S_{10}	$Fe_{50}S_{50}$

The core and 'rim' compositions show some variations but they match compositions across the gap (*cf.* Fig. 1).

Allocation C2054,0,35,24,1 from the same track contains high-Ni, Fe-Ni-S grains that include a 70-nm size euhedral grain, $Fe_{46}Ni_{47}S_7$, with a discontinuous rim, $Fe_{21}Ni_6S_{73}$ that are the most Ni-rich compound present. FeS is also present. A tie between the core and rim compositions line intersects the Fe-S join at FeS_4 and the Fe-Ni join at Fe/Ni (at) = 1. This core-mantle grain is an example of a surviving fragment or the entire original Wild 2 Fe,Ni-metal grain that had acquired a layer of FeS_4-rich melt or vapor-phase condensate.

NOTE: Fe-Ni-S compositions were hand-plotted in Figs 1 & 2 lacking a digitized template of the Fe-Ni-S ternary.

Conclusions: The current Fe-S diagram at S>60 at% has no liquidus relationships for FeS_2 and FeS_4 and no opportunity to separate FeS_2 and FeS_4 melt across the range of immiscible liquids field. The compositions (Figs. 1 & 3) support both liquidus-controlled and deep metastable eutectic processes during quenching. Given the reducing conditions during Stardust hypervelocity capture [5] the Fe-S-Si ternary system with a vast miscibility gap at 1 atm will be relevant. Experiments defining the miscibility gap found that droplets of 'FeS' melt were suspended in the other 'Fe-Si' liquid. It explains the shotgun pattern of the Fe-Ni-S compounds in silica glass with background level Fe. The Fe-S melts in the experiments [9] are ~40 and 50 at% S (Si-free) and ~30 at% S (Si present) that (fortuitously) match the Fe-S gap.

The observed discontinuous zoning might be a liquid-in-liquid feature with compositions across the gap and between Ni-bearing and Ni-free Fe-S melts or condensed-liquids. This zoning is a primary feature and not due to chemical diffusion during quenching albeit that the latter cannot be fully excluded.

The composition of Wild 2 sulfides that didn't survive should be the mean of the measured composition, *viz.* $Fe_{70}Ni_{3.5}S_{26.5}$ (Fig. 1) and $Fe_{59}Ni_4S_{37}$ (Fig. 2). Assuming original pyrrhotite grains ~50-70% of sulfur is missing but the missing mass is very small.

References: [1] Ishii H. A. et al. (1997) *Nature, 90,* 1151–1154. [2] Hörz F. et al. (2009) *Meteoritics & Planet. Sci., 44,* 1243-1264. [3] Rietmeijer F. J. M. (2009) *Meteoritics & Planet. Sci., 44,* 1121-1132. [4] Rietmeijer F. J. M. (2009) *Meteoritics & Planet. Sci., 44,* 1589-1609. [5] Rietmeijer F. J. M. et al. (2008) *Meteoritics & Planet. Sci., 43,* 121-134. [6] Hsieh K.-C. et al. (1987) *High Temp. Sci., 23,* 17-38. [7] Leroux H. et al. (2008) *Meteoritics & Planet. Sci.,* 43, 97-120. [8] Burns R. G. & Fisher D. S. (1994) *Hyperfine Interactions, 91,* 571-576. [9] Sanloup C. & Fei Y. (2004) *Phys. Earth Planet. Inter., 147,* 57-65. This work was supported by NNX07AM65G, NASA Stardust Analyses Program.